Molecular Crystals and Liquid Crystals

Publication details, including instructions for authors and subscription information:
http://www.tandfonline.com/loi/gmcl20

Holographic and Nonholographic Organic-Inorganic Hybrids

D. R. Evans [a] , G. Cook [a b] & J. L. Carns [a c]

[a] Air Force Research Laboratory, Materials and Manufacturing Directorate, Wright-Patterson Air Force Base, Ohio, USA

[b] Universal Technology Corporation, Dayton, Ohio, USA

[c] General Dynamics Information Technology, Dayton, Ohio, USA

Version of record first published: 22 Sep 2010

To cite this article: D. R. Evans, G. Cook & J. L. Carns (2008): Holographic and Nonholographic Organic-Inorganic Hybrids, Molecular Crystals and Liquid Crystals, 488:1, 190-201

To link to this article: http://dx.doi.org/10.1080/15421400802218538

Mol. Cryst. Liq. Cryst., Vol. 488, pp. 190–201, 2008

ISSN: 1542-1406 print/1563-5287 online
DOI: 10.1080/15421400802218538

Taylor & Francis
Taylor & Francis Group

Holographic and Nonholographic Organic–Inorganic Hybrids

D. R. Evans[1], G. Cook[1,2], and J. L. Carns[1,3]
[1]Air Force Research Laboratory, Materials and Manufacturing Directorate, Wright-Patterson Air Force Base, Ohio, USA
[2]Universal Technology Corporation, Dayton, Ohio, USA
[3]General Dynamics Information Technology, Dayton, Ohio, USA

In this article, we review the concepts of holographic and nonholographic organic-inorganic hybrids, both comprising a liquid crystal layer adjacent to inorganic crystalline windows. Photo-generated fields from photorefractive (holographic) or photovoltaic (nonholographic) crystalline windows govern the orientation of the liquid crystal molecules in the hybrid cells. Holographic hybrids have been used to demonstrate a high gain Bragg-matched beam coupling, whereas nonholographic hybrids have been used to demonstrate a lensing effect.

Keywords: hybrids; liquid crystal; photo refractive; photovoltaic

I. INTRODUCTION

Recent work has shown that hybridizing organic liquid crystals (LCs) with inorganic crystals, such as photorefractive or photovoltaic (PV) crystalline windows, can add considerable benefit to the operation and the performance of LC devices [1–7]. Effects such as photorefractive beam coupling, lensing, and birefringence switching can be activated without the need of externally applied fields. These effects have been shown to be enhanced in organic-inorganic hybridized cells when compared to ordinary LC or LC-polymer hybrid devices.

Two types of organic-inorganic hybrids have been explored: photorefractive (holographic) hybrids and photovoltaic (nonholographic) hybrids. These two areas will be reviewed in this paper from the perspective of Bragg-matched beam coupling in the photorefractive hybrids [1,2]

Address correspondence to D. R. Evans, Air Force Research Laboratory, Materials and Manufacturing Directorate, Wright-Patterson Air Force Base, Ohio, 45433, USA. E-mail: dean.evans@wpafb.af.mil

and lensing in PV hybrids [4,5]. The mechanisms involved and methods for improving each of these concepts are discussed. Variations of these structures have been explored in ferroelectric nanoparticle doped photorefractive hybrids, resulting in an enhancement of the gain coefficient; and twisted nematic hybrid structures between crossed-polarizers, resulting in birefringence switching in PV hybrid light-valves. These modified hybrids will not be discussed in this review, but details of our work in these areas can be found in Refs. [4,8].

II A. PHOTOREFRACTIVE HOLOGRAPHIC HYBRIDS – BACKGROUND

Photorefractive two-beam coupling (TBC) enables *uni-directional* transfer of power from one beam to another. Several classes of photorefractive materials have been studied over the years for beam coupling applications: inorganic crystals [9], polymers [10,11], and LCs [12]. For inorganic crystals, the exponential gain coefficient is generally in the range of 10 to $100\,cm^{-1}$, with the highest being observed in $LiNbO_3$:Fe,Tb [13]. These gain coefficients are governed by the relatively small modulation in refractive index (approximately 10^{-4}), which is limited by the magnitude of the space-charge field and the electro-optic coefficients.

From a pure organic perspective, nematic LCs reoriented by photogenerated space charges in adjacent polymer photorefractive [14] or photoconducting layers [15,16] have been explored, where the latter reports a record gain coefficient of $3700\,cm^{-1}$ in the Raman-Nath regime (two orders of magnitude higher than those typically seen in solid inorganic crystals). Although the gain coefficients can be very large in organic photorefractives owing to molecular reorientation, TBC in these devices has limitations since they only operate in the Raman-Nath regime; in this case beam coupling results in multiple order diffracted beams and restricts the angle between the pump and signal beams to less than a few degrees. Although large gain coefficients are observed in other types of organic-inorganic devices [6,7], they have been so far limited to the Raman-Nath regime (although the nature of this limitation is not understood) and the coupling is purely diffractive (i.e. not a uni-directional power transfer, rather they are always in the direction from the strong beam to the weak beam; there is zero gain when the beams are equal intensities–unlike the photorefractive hybrid described in this paper).

In our research, we have achieved very large LC gain coefficients for the Bragg regime, where the space-charge field originated from the inorganic photorefractive crystals used as windows for

undoped nematic LC cells [2]. In these devices the grating period is much smaller than the LC layer thickness. A variation of this concept was first proposed nearly a decade ago in a theoretical paper that suggested the evanescent field from a space-charge field inside a single photorefractive window could reorient LC molecules [17]. A variation of this concept was suggested and demonstrated in a dual window device (hybrid organic-inorganic photorefractive device), which allowed uni-directional beam-coupling [18,1].

In hybrid organic-inorganic photorefractive devices (holographic hybrids) the evanescent field from the inorganic windows, which penetrates approximately 1.5 times the grating spacing distance [18], exerts a torque on the nearby LC molecules. The electric torque modulates the LCs, causing them to align with the periodic space-charge field. This results in a modulated refractive index that is 90 degrees out-of-phase with respect to the initial interference pattern, as governed by the inorganic windows; this enables photorefractive beam coupling. The beam coupling occurs in the organic LC layer, which is known to have a large gain coefficient. The small trap density in LCs (and polymers) is complemented by the large trap density (a requirement for Bragg-matched coupling) of the inorganic photorefractive windows. The required conditions to achieve Bragg-matched coupling using simple photorefractive diffusion gratings and undoped nematic LCs are explained in section II B.

II B. PHOTOREFRACTIVE HOLOGRAPHIC HYBRIDS – DISCUSSION

The holographic hybrid cells comprise a LC layer, TL205 or a similar nematic LC, between two photorefractive SBN:Ce windows. Details of the device preparation and the experimental procedure can be found in Refs. [2,3]. The holographic hybrid cell was placed at the overlap of pump and signal beams, which were generated by a 532 nm CW Verdi laser and a series of beam splitters and mirrors. The cell was placed approximately normal to the bisector of the two beams with the c-axis of each window in the plane of the incident polarization. A large separation angle between the beams was used (approximately 20 degrees is optimum in our samples). The orientation of the c-axes of the SBN:Ce windows allowed the signal beam to be amplified; the transmitted pump and signal beam powers were monitored with a power meter. The measured gain is defined as the power of the signal beam with the pump beam present divided by the transmitted signal beam in the absence of the pump beam. For each grating spacing the gain of the LCs was determined by dividing the gain for

the cell filled with LCs by the gain of the cell filled with oil. The gain coefficient, Γ for the LC layer is given by:

$$\Gamma = \frac{1}{d}\log_e(G) \tag{1}$$

where G is the small signal gain and d is thickness of the LC layer. Note that unlike pure organic photorefractive materials (polymers or LCs), there is no applied electric field. The required field is the evanescent field resulting from the photoactivated space-charge field inside the inorganic photorefractive windows.

There are two conditions required to achieve Bragg-matched TBC in holographic hybrid cells: (1) the LC alignment must be asymmetric and (2) the LC molecules must be sensitive to the *sign* of the space-charge field (i.e. the evanescent field). A demonstration of Bragg-matched TBC in a holographic hybrid device can be seen in Figure 1. Neither condition is met in regular glass cells where there is a symmetrical molecular alignment of the nematic LCs and no sensitivity to the sign of the electric field [2,3]. In order to achieve the same spatial frequency of the refractive index grating as the optical interference pattern (i.e. condition for Bragg matched optical amplification), the cells must have a broken symmetry. This has been shown to be achieved by inducing a pretilt in the LC layer [2,19].

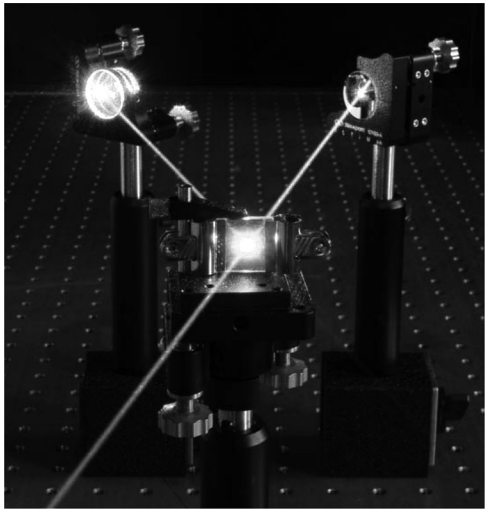

FIGURE 1 Bragg-matched two-beam coupling in a holographic hybrid organic-inorganic photorefractive cell comprising a LC layer (TL205) between two SBN:Ce windows.

The pretilt, believed to be the result of Van der Waal's forces between the inorganic SBN:Ce windows and the LC molecules [20], does more than just break the symmetry in the molecular alignment (as described above); it also induces a flexopolarization generating an induced dipole in the nematic LCs giving them their sensitivity to the sign of the electric field (this is not the case for nematics that are not splayed). Both the pretilt and flexoelectric effects were determined experimentally [2]. The pretilt was measured using a common technique modified for birefringent windows [19], and found to have up to a 16 degree pretilt of the LC director. The flexoelectric effect was determined by measuring the gain coefficient for: (1) different window orientations (rubbing directions/orientations with respect to the c-axes) and (2) cells with various LC layer thicknesses. With an ordinary LC cell (glass windows): (1) one would not expect a change

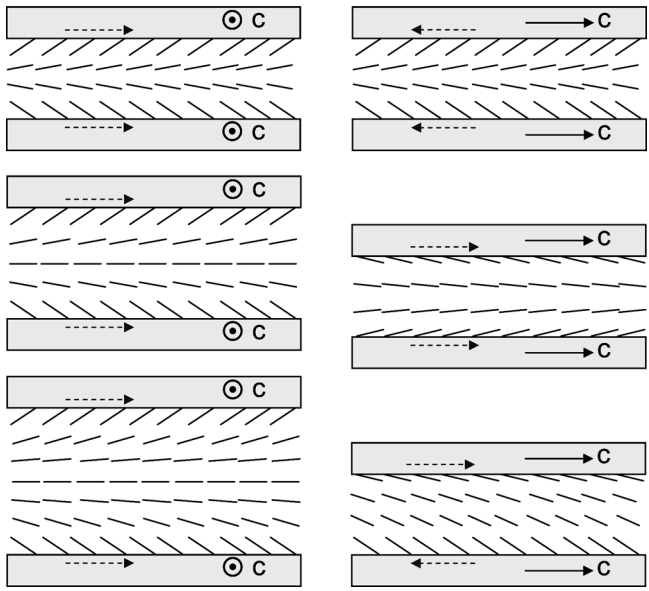

FIGURE 2 Diagrams of the LC molecular orientation (splay and bend) in photorefractive hybrid cells and their dependence on cell orientation, rubbing direction, and cell thickness. (Left Column) Constant rubbing direction (orthogonal to the SBN:Ce c-axes) with varying thickness. The gain coefficient decreases from top to bottom. (Right Column) Constant thickness with varying rubbing directions (parallel and anti-parallel to the SBN:Ce c-axes). The gain coefficient decreases from top to bottom. The dashed arrows indicate the rubbing direction.

in the gain for different window/rubbing orientations and (2) one would not expect the gain to increase with a decrease in the gain layer thickness. Completely different results were observed for both cases, when the crystalline windows were used in place of glass windows. Parallel rubbing of each SBN:Ce window aligned the LC molecules such that a splay alignment was maximized, while anti-parallel rubbing resulted in a bend of the LC molecules resulting in a reduced gain. There was also a strong dependence for rubbing along the c-axis or orthogonally to c-axis [2]. A comparison of several hybrid cell configurations showed that the magnitude and the direction of gain varied with cell orientation and rubbing direction; this suggested that the flexoelectric effect played a role in the beam coupling [2]. In addition an unusual thickness dependence, where thinner LC layers resulted in a higher gain, which also suggested that the flexoelectric was responsible for the large gain. The maximizing and minimizing of the splay effect (i.e. flexopolarization) by varying the cell orientation and thickness can be seen in diagrams in Figure 2. The actual gain (G) as a function of grating spacing for three different LC layer thicknesses can be seen in Figure 3. Results of the gain coefficient as a function of cell orientation/rubbing direction can be found in Refs. [2,3].

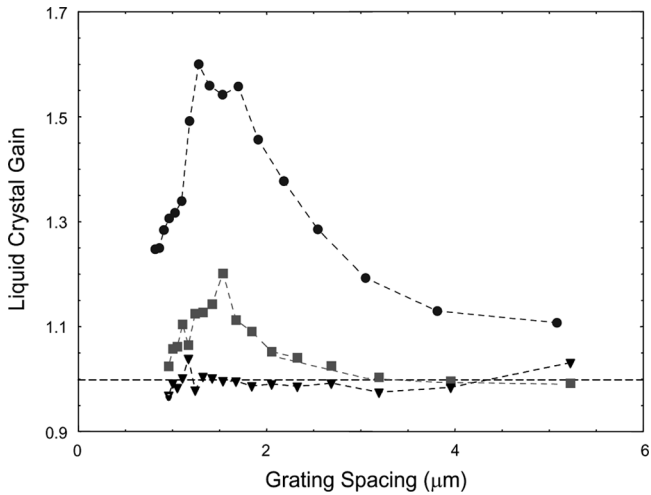

FIGURE 3 Gain (G) as a function of grating spacing for three different LC layer thicknesses: 10 μm cell (circles) yields a large gain, 20 μm (squares) yields a moderate gain, and 38 μm (triangles) yields a small gain. The degree of splay is depicted for each thickness in Figure 2 (Left Column).

III A. PHOTOVOLTAIC NONHOLOGRAPHIC HYBRIDS – BACKGROUND

The concept of a PV nonholographic hybrid is similar to the holographic photorefractive hybrid, although it is less complex. These devices also utilize an internally generated, photo-induced electric field; but it is a bulk field, not a complex periodic space-charge field with requirements of a broken symmetry and sensitivity to the sign of the electric field. When a pure LC layer is placed between PV windows, the LC molecules can be reoriented such that the director aligns itself with the uniform electric field. Note other effects can produce internal fields, e.g. pyroelectric, piezoelectric, etc. We have chosen to work with the PV effect, because it is relatively easy to predict and control the field behavior.

One of the more common PV crystals is $LiNbO_3$:Fe, which is capable of producing a bulk electric field greater than 100 kV/cm [21,22]. The PV effect is activated upon illumination, where an asymmetrical potential associated with the material causes photoionized electrons to move in a preferential direction giving rise to a photo-induced current and a subsequent electric field. We have demonstrated that a PV field generated in $LiNbO_3$:Fe windows can efficiently reorient LC molecules [4,5]. When exposed to a wavelength of light which promotes photoionization (see the broad absorption spectrum of Fe^{2+} in $LiNbO_3$ in Ref. [25]), the surfaces charges resulting from the induced photocurrent generate a field across the LC layer sufficient to reorient the LC molecules. Evidence of the large charge build up at the surface of $LiNbO_3$:Fe crystals, which can even result in the ionization of the surrounding air, can be found in Refs. [23,24].

III B. PHOTOVOLTAIC NONHOLOGRAPHIC HYBRIDS – DISCUSSION

Various types of PV operated devices have been explored for spatial filtering. These nonholographic hybrid cells are constructed with planarly aligned nematic LCs between: (1) two PV windows, (2) one PV window and one uncoated glass window, or (3) one PV window and one ITO (indium tin oxide–transparent conductive coating throughout the visible spectral region) coated glass window. For the nonholographic PV hybrids, a lensing effect is the primary mechanism for spatial filtering. The photorefractive effect is a secondary mechanism, which creates counter-propagating TBC [4,5,26]. This is not a detrimental effect, but it is noted since it is unrelated to the presence of LC molecules.

The details of the construction of the PV hybrids can be found in Refs. [4,5]. For all our PV hybrids, $LiNbO_3$:Fe (0.05 molar % Fe_2O_3) windows were used with the c-faces (XY plane) polished. The thickness of each crystalline window along c-axis was 1.0 mm. The cells were constructed with the windows enclosing a planarly aligned nematic LC layer, where the windows were rubbed anti-parallel with respect to one another (in contrast to the holographic hybrid cell preparation).

A diagram of the PV hybrid structure is shown in Figure 4. In Figure 5, the transmitted intensity as a function of time for the PV hybrid is plotted for two cases: 1) the cell filled with oil for a reference trace and 2) the cell filled with planarly aligned nematic LCs. In both measurements, an aperture is placed behind the cell in the far field. The trace showing a gradual reduction in transmitted intensity with time is the reference cell; this reduction is solely related to the photorefractive effect. i.e. counter-propagating TBC. Note, this effect of beam depletion can be eliminated by propagating the beam in the opposite direction. When introducing a LC layer between the PV windows, the reduction in the transmitted beam occurs much more rapidly; although within the first second of exposure the transmitted intensity temporarily increases, which is then followed by a subsequent reduction of the intensity. This is attributed to a lensing effect, which is a result of the Gaussian profile of the incident beam intensity. The build up of surface charges on the $LiNbO_3$:Fe windows and the field generated across the LC layer is initially strongest in the

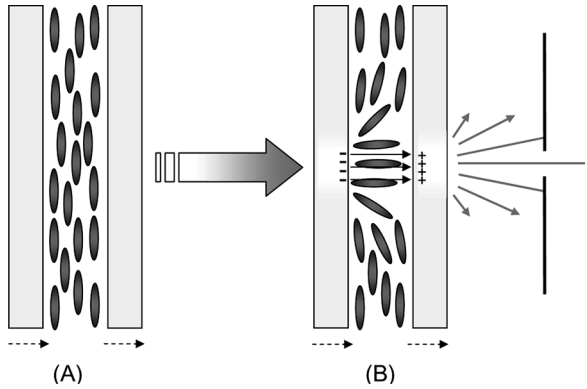

FIGURE 4 Diagram of the nonholographic PV hybrid structure comprising a LC layer (TL205) between two $LiNbO_3$:Fe windows: (A) without light and (B) with light. In case B, the PV field lines are shown between the PV windows; an aperture is placed in the far field. The dotted lines indicate the direction of the c-axes.

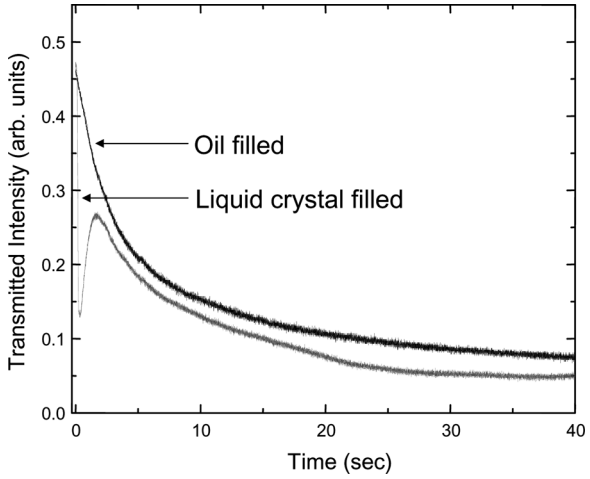

FIGURE 5 Transmitted intensity as a function of time for oil filled and LC filled PV cells.

center of the Gaussian beam, so there is a greater influence on the LC director reorientation here than at the edges of the beam.

The lensing effect is strongly depended on having a Gaussian-like refractive index profile (a result of having a Gaussian-like distribution of the surface charges); for this reason we explored the difference in the PV hybrid performance by replacing the rear PV window with an uncoated glass window. The performance of this configuration was evaluated against the PV hybrid cell comprising the PV windows in the front and an ITO coated glass window in the rear. For the sake of comparison, the rear PV window was placed adjacent to the front PV window such that the full TBC contribution was still present. Figure 6 shows PV hybrid cell diagrams and the spatial distribution of the transient and steady state refractive indices. The shaded region represents the portion of the cell illuminated by the laser beam. The main difference of having an uncoated window rather than an ITO coated window is that the field lines are strongly divergent. Although both types of cells (uncoated and ITO coated glass rear windows) yield a graded index of refraction in the transient regime, the steady state regime was very different.

In the steady state, the type of glass window plays a significant role. Once the surface charges have built up, the refractive index becomes homogenous in the cell with the rear ITO coated glass; the lensing effect is minimized and the divergence of the transmitted beam is dramatically reduced. This is the same explanation that was given above

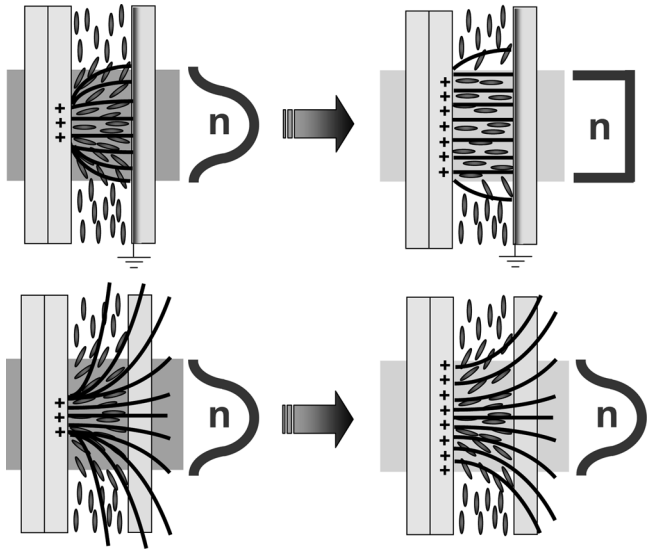

FIGURE 6 PV hybrid cell with both PV windows in the front and a glass window in the rear: (Top) ITO coated glass and (Bottom) uncoated glass. The spatial distribution of the refractive indices is shown for: (Left) the transient state and (Right) the steady state.

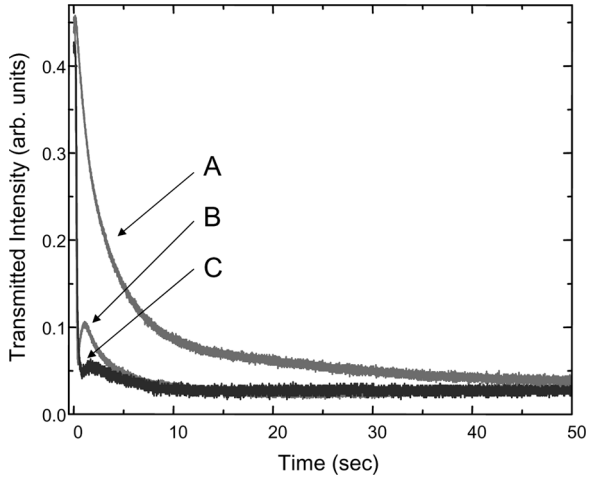

FIGURE 7 Transmitted intensity as a function of time: (A) oil filled PV hybrid, (B) modified hybrid structure with two PV windows in the front and one ITO coated window in the rear, and (C) modified hybrid structure with two PV windows in the front and one uncoated window in the rear.

for the case of the nonholographic hybrids comprised of two PV windows, where an increase in transmitted intensity was observed within the first second of illumination. This case performed more like the cell with the ITO coated glass on the rear (more conductive) than the one with the uncoated glass on the rear (non/weakly conductive).

In order to maximize the lensing effect, the strongly diverging field lines and hence the Gaussian refractive index profile in the steady state are required. Figure 7 shows the effect that the uncoated and ITO coated glass windows have on the PV hybrid performance. The lensing effect remains strong in the steady state regime for the case of the PV hybrid cell with the uncoated glass. The typical decrease in performance (increase in transmitted intensity) as seen in both the two PV window (front and rear) and rear ITO coated glass window devices, has been dramatically improved by using a simple uncoated glass window on the rear of the PV hybrid cell.

IV. SUMMARY

Holographic (organic-inorganic) photorefractive hybrids, comprising photorefractive crystalline windows (SBN:Ce) and a LC layer, yield large gain coefficients in the Bragg regime. Two conditions are required in order to have Bragg matched TBC in holographic hybrid devices: (1) a broken molecular symmetry and (2) a LC sensitivity to the *sign* of the electric field. Both conditions are met as a result of a pretilt of the LC alignment. The pretilt is believed to be a result of intermolecular forces between the SBN:Ce windows and the LC molecules. In addition to breaking the symmetry, the pretilt (splay) generates a flexoelectric effect, which induces an electric dipole in the nematic LCs causing them to be sensitive to the sign of the electric field.

Nonholographic (organic-inorganic) photovoltaic hybrids, comprising PV crystalline windows ($LiNbO_3$:Fe) and glass windows have been shown to reorient the LC director through an internally generated electrical field. Maximizing the lensing effect to enhance spatial filtering was achieved by using an uncoated glass window on the rear of the PV hybrid cell in order to maintain a Gaussian refractive index profile in the steady state regime.

REFERENCES

[1] Cook, G., Wyres, C. A., Deer, M. J., & Jones, D. C. (2003). *SPIE*, *5213*, 63.
[2] Cook, Carns, J. L., Saleh, M. A., & Evans, D. R. (2006). *Mol. Cryst. Liq. Cryst.*, *453*, 141.
[3] Evans, D. R. & Cook, G. (2007). *J. of Nonlin. Opt. Phys. and Mat.*, *16*, 271.

[4] Carns, J. L., Cook, G., Saleh, M. A., Serak, S. V., Tabiryan, N. V., & Evans, D. R. (2006). *Opt. Lett.*, *31*, 993.
[5] Carns, J. L., Cook, G., Saleh, M. A., Basun, S. A., Serak, S. V., Tabiryan, N. V., & Evans, D. R. (2006). *Mol. Cryst. Liq. Cryst.*, *453*, 83.
[6] Aubourg, P., Huignard, J.-P., Hareng, M., & Mullen, R. A. (1982). *Appl. Opt.*, *21*, 3706.
[7] Residori, S., Bortolozzo, U., Montina, A., Arechhi, F. T., & Huignard, J.-P. (2007). *J. of Nonlin. Opt. Phys. and Mat.*, *16*, 343.
[8] Cook, G., Glushchenko, A. V., Reshetnyak, V., Griffith, A. T., Saleh, M. A., & Evans, D. R. (2008). *Opt. Exp.*, *16*, 4015.
[9] Solymar, L., Webb, D. J., & Grunnet-Jepsen, A. (1996). *The Physics and Applications of Photorefractive Materials*, Clarendon Press: Oxford.
[10] Sutter, K. & Günter, P. (1990). *J. Opt. Soc. Am. B*, *7*, 2274.
[11] Sutter, K., Hullinger, J., & Günter, P. (1990). *Solid State Commun.*, *74*, 867.
[12] Khoo, I. C., Guenther, B. D., Wood, M. V., Chen, P., Shih, Min-Yi. (1997). *Opt. Lett.*, *22*, 1229.
[13] Cook, G., Finnan, C. J., & Jones, D. C. (1999). *Appl. Phys. B*, *68*, 911.
[14] Brignon, A., Bongrand, I., Loiseaux, B., & Huignard, J. P. (1997). *Opt. Lett.*, *22*(24), 1855.
[15] Kajzar, F., Bartkiewicz, S., & Miniewicz, A. (1999). *Appl. Phys. Lett.*, *74*, 2924.
[16] Bartkiewicz, S., Matczyszyn, K., Miniewicz, A., & Kajzar, F. (2001). *Opt. Commun.*, *187*, 257.
[17] Tabiryan N. V. & Umeton, C. (1998). *J. Opt. Soc. Am. B*, *15*, 1912.
[18] Jones, D. C. & Cook, G. (2004). *Opt. Commun.*, *232*, 399.
[19] Sutherland, Richard L., Cook, Gary & Evans, Dean R. (2006). *Opt. Express*, *14*, 5365.
[20] Alexe-Ionescu, A. L., Barberi, R., Bonvent, J. J., & Giocondo, M. (1996). *Phys. Rev. E*, *54*, 529.
[21] Glass, A. M., von der Linde, D., & Negran, T. J. (1974). *Appl. Phys. Lett.*, *25*, 233.
[22] Cook, G., Duignan, J. P., & Jones, D. C. (2001). *Opt. Commun.*, *192*, 393.
[23] Evans, D. R., Basun, S. A., Saleh, M. A., Pottenger, T. P., Cook, G., Bunning, T. J., & Guha, S. (2002). *IEEE J. Quantum. Elec.*, *38*, 1661.
[24] Evans, D. R., Gibson, J. L., Basun, S. A., Saleh, M. A., & Cook, G. (2005). *Opt. Materials*, *27*, 1730.
[25] Basun, S. A., Evans, D. R., Barnes, J. O., Bunning, T. J., Guha, S., Cook, G., & Meltzer, R. S. (2002). *J. Appl. Phys.*, *92*, 7051.
[26] Carns, J. L., Cook, G., Saleh, M. A., Holmstrom, S. A., Guha, S., & Evans, D. R. (2005). *Appl. Opt.*, *44*, 7452.